0026-895X/03/6304-799–807$7.00
MOLECULAR PHARMACOLOGY
Copyright © 2003 The American Society for Pharmacology and Experimental Therapeutics
Mol Pharmacol 63:799–807, 2003

Vol. 63, No. 4
2211/1052153
Printed in U.S.A.

Brominated Derivatives of Noscapine Are Potent Microtubule-interfering Agents That Perturb Mitosis and Inhibit Cell Proliferation

JUN ZHOU, KAMLESH GUPTA, SHEFALI AGGARWAL, RITU ANEJA, RAMESH CHANDRA, DULAL PANDA, and HARISH C. JOSHI

Graduate Program in Biochemistry, Cell and Developmental Biology (J.Z.) and Department of Cell Biology (J.Z., H.C.J.), Emory University, Atlanta, Georgia; Bhupat and Jyoti Mehta School of Biosciences and Bioengineering, Indian Institute of Technology, Bombay, Mumbai, India (K.G., D.P.); Dr. B. R. Ambedkar Center for Biomedical Research (S.A., R.C.) and Department of Chemistry (R.A.), University of Delhi, Delhi, India

Received October 11, 2002; accepted December 16, 2002

This article is available online at http://molpharm.aspetjournals.org

ABSTRACT

Noscapine, a microtubule-interfering agent, has been shown to arrest mitosis, to induce apoptosis, and to have potent antitumor activity. We report herein that two brominated derivatives of noscapine, 5-bromonoscapine (5-Br-nosc) and reduced 5-bromonoscapine (Rd 5-Br-nosc), have higher tubulin binding activity than noscapine and affect tubulin polymerization differently from noscapine. In addition, they are able to arrest cell cycle progression at mitosis at concentrations much lower than noscapine. Interestingly, whereas noscapine-arrested cells have nearly normal bipolar spindles, cells arrested by 5-Br-nosc and Rd 5-Br-nosc form multipolar spindles. Nevertheless, noscapine and the two derivatives all affect the attachment of chromosomes to spindle microtubules and they impair the tension across paired kinetochores to similar degrees. 5-Br-nosc and Rd 5-Br-nosc are also more active than noscapine in inhibiting the proliferation of various human cancer cells, including those that are resistant to paclitaxel and epothilone. Our results thus indicate a great potential for the use of 5-Br-nosc and Rd 5-Br-nosc both as biological tools for studying microtubule-mediated processes and as chemotherapeutic agents for the treatment of human cancers.

Microtubules are helical polymers assembled from the heterodimer of α- and β-tubulin. They play important roles in shaping cells and directing intracellular motility. During cell division, microtubules form a bipolar apparatus called the mitotic spindle, which mediates chromosome distribution into two daughter cells (McIntosh, 1994). Microtubules are intrinsically dynamic and they alternate abruptly and stochastically between periods of growth and shortening. The dynamic nature is crucial for the organization and function of microtubules, especially for spindle morphogenesis and chromosome movement during mitosis (Desai and Mitchison, 1997). Eukaryotic cells have evolved a surveillance mechanism called the spindle assembly checkpoint, which blocks cell cycle progression at mitosis when the spindle has a defect or when chromosomes are not properly aligned at the equatorial plane (Zhou et al., 2002d). Not surprisingly, chemical compounds that target microtubules can arrest cells at mitosis, a property attributed to the use of microtubule-interfering agents in cancer chemotherapy (van Tellingen et al., 1992; Rowinsky, 1997; Crown and O'Leary, 2000).

There are two classes of microtubule-interfering agents: those that inhibit microtubule polymerization (such as colchicine, nocodazole, and the vinca alkaloids) and those that promote microtubule polymerization, such as the taxoids and epothilone (Jordan and Wilson, 1999). It is now clear that although all of these agents can efficiently block cell cycle progression, only a select few have been used clinically for the treatment of human cancers. In addition, there are differences regarding the toxicity and the efficacy of these antimicrotubule agents for distinct classes of tumors. Even for drugs that are currently in clinical use (e.g., paclitaxel and vinblastine), although patients have impressive initial response, many of them relapse after treatment because of the development of drug resistance. Thus, the development of more potent and selective antimicrotubule drugs are greatly needed, especially for the treatment of human cancers resistant to currently used drugs.

We have recently identified noscapine (Fig. 1A), a phthalideisoquinoline alkaloid from opium, as a microtubule-inter-

This work was supported by funding from the National Institutes of Health (to H.C.J.) and from the Department of Science and Technology, Government of India (to D.P.).

ABBREVIATIONS: 5-Br-nosc, 5-bromonoscapine; Rd 5-Br-nosc, reduced 5-bromonoscapine; FBS, fetal bovine serum; PIPES, piperazine-*N*,*N*′-bis(2-ethanesulfonic acid); PBS, phosphate-buffered saline; PI, propidium iodide; DMSO, dimethyl sulfoxide; FITC, fluorescein isothiocyanate.

fering agent that binds stoichiometrically to tubulin and alters tubulin conformation (Ye et al., 1998). Like many other antimicrotubule agents, noscapine suppresses the dynamics of microtubule assembly, blocks cell cycle progression at mitosis, and then causes apoptotic cell death in many cancer cell types (Ye et al., 1998, 2001; Zhou et al., 2002a, 2002b). Noscapine inhibits the progression of murine lymphoma, melanoma, and human breast tumors implanted in nude mice with little or no toxicity to the kidney, heart, liver, bone marrow, spleen, or small intestine and does not inhibit primary humoral immune responses in mice (Ye et al., 1998; Ke et al., 2000; Landen et al., 2002). The water solubility and feasibility for oral administration are also very valuable advantages of noscapine over many other antimicrotubule drugs (Dahlstrom et al., 1982; Haikala et al., 1986; Karlsson et al., 1990). In this study, we demonstrate that two brominated noscapine derivatives, 5-bromonoscapine (5-Br-nosc; Fig. 1D) and reduced 5-bromonoscapine (Rd 5-Br-nosc; Fig. 1G), are more potent microtubule-interfering agents that arrest mitosis and inhibit cell proliferation with much higher efficiency than noscapine.

Materials and Methods

Materials. Goat brain microtubule proteins were isolated in the presence of 1 M glutamate by two cycles of polymerization and depolymerization (Hamel and Lin, 1981). Tubulin was purified from the microtubule proteins by phosphocellulose chromatography as described previously (Panda et al., 2000; Joshi and Zhou, 2001), and the concentration of tubulin was determined by the method of Bradford (1976) using bovine serum albumin as a standard. The tubulin solution was stored at −80°C until future use. Paclitaxel and nocodazole were purchased from Sigma (St. Louis, MO), and noscapine (97% purity) was from Aldrich (Milwaukee, WI).

Preparation of Brominated Derivatives of Noscapine. 5-Br-nosc (1,3-dihydro-4,5-dimethoxy-1-[1,2,3,4-tetrahydro-5-bromo-8-methoxy-2-methyl-6,7-methylendioxy-isoquinolyl-1]isobenzofuran-

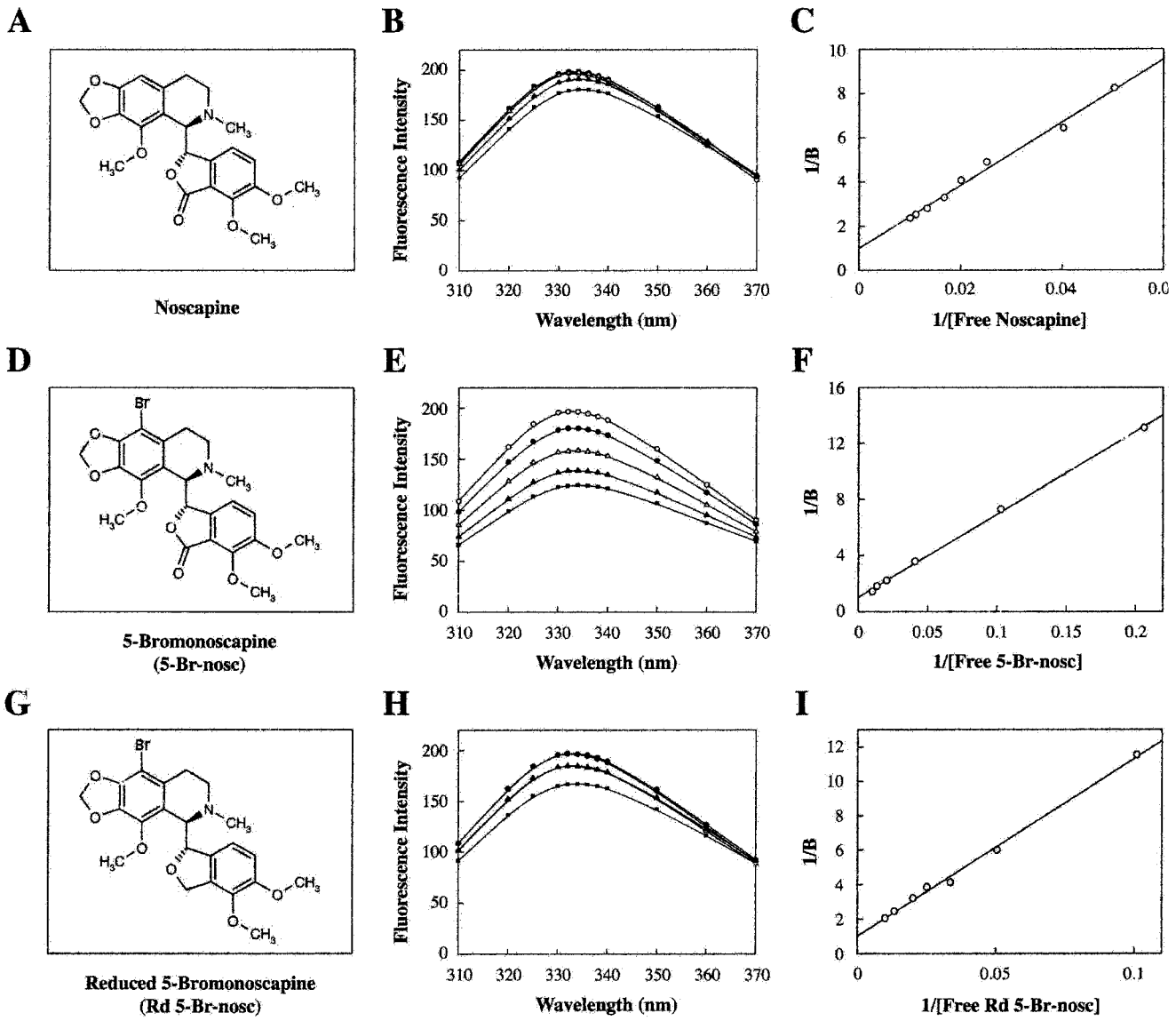

Fig. 1. Fluorescence quenching of tubulin by noscapine and its two derivatives, 5-Br-nosc and Rd 5-Br-nosc. A, D, and G show the molecular structures of noscapine, 5-Br-nosc, and Rd 5-Br-nosc, respectively. The tubulin fluorescence emission spectrum is quenched by noscapine (B), 5-Br-nosc (E), and Rd 5-Br-nosc (H) in a concentration-dependent manner. C, F, and I are double reciprocal plots showing a dissociation constant (K_d) of 144 ± 2.8 μM for noscapine binding to tubulin (C), 54 ± 9.1 μM for 5-Br-nosc binding to tubulin (F), and 106 ± 4.2 μM for Rd 5-Br-nosc binding to tubulin (I).

3-one) and Rd 5-Br-nosc (1,3-dihydro-4,5-dimethoxy-1-[1,2,3,4-tetrahydro-5-bromo-8-meth-oxy-2-methyl-6,7-methylendioxy-isoquinolyl-1]isobenzofuran) were prepared as described previously with minor modifications (Dey and Srinivasan, 1935). Briefly, noscapine was dissolved in 48% HBr solution, and Br_2/H_2O was added to this solution until no semisolid precipitate formed. The supernatant liquid was decanted to another flask, and NH_3 solution was added to the semisolid precipitate to form solid precipitate. The supernatant liquid was also neutralized to pH 10 to form solid precipitate. The two solid precipitates were combined and recrystallized with ethanol to produce 5-Br-nosc. Yield, 75%; melting point; 169 to 170°C; calculated percentage (found percentage), C, 53.67 (53.62); H, 4.50 (4.44); N, 2.85 (2.71). IR, 2945 (m), 2800 (m), 1759 (s), 1612 (m), 1500 (s), 1443 (s), 1263 (s), 1091 (s), 933 (w) cm^{-1}. ^1H NMR ($CDCl_3$, 300 MHz), δ 7.04 (d, J = 7 Hz, 1H), 6.32 (d, J = 7 Hz, 1H), 6.03 (s, 2H), 5.51(d, J = 4 Hz, 1H), 4.55 (d, J = 4 Hz, 1H), 4.10 (s, 3H), 3.98 (s, 3H), 3.89 (s, 3H), 2.52 (s, 3H), 2.8 to 1.93 (m, 4H). Mass spectrometry: fast atom bombardment ions, *m/z* (relative abundance percentage), 494 (93.8), 492 (100), 300 (30.5), 298 (35.4); matrix-assisted laser desorption ionization ions, *m/z* 491.37 $(M)^+$, 493.34; electrospray ionization/tandem mass spectrometry, parent ion masses, 494, 492; daughter ion masses (intensity, percentage): 433 (51), 431 (37), 300 (100), 298 (93.3). Rd 5-Br-nosc was prepared by using the same procedure as for 5-Br-nosc, except that the reduced form of noscapine was used as the starting material. Yield, 70%; melting point, 113 to 114°C; calculated percentage (found percentage), C, 55.24 (55.19); H, 5.05 (5.25); N, 2.93 (2.88). ^1H NMR ($CDCl_3$, 300 M Hz), δ 6.73 (d, J = 8Hz, 1H), 6.11 (d, J = 8Hz, 1H), 6.08 (s, 2H), 5.78 (s, 2H), 5.33 (dd, J = 12Hz, 1H), 5.05 (dd, J = 12Hz, 1H), 4.90 (s, 1H), 3.86 (s, 6H), 3.83 (s, 3H), 3.42 to 3.19 (m, 2H), 2.99 (s, 3H), 2.82 to 2.80 (m, 2H). Infrared, 2950 (m), 2852 (m), 1635 (w), 1616 (m), 1450 (s), 1267 (s), 1226 (s), 1078 (s), 1035 (s) cm^{-1}. Mass spectrometry: fast atom bombardment ions, *m/z* (relative abundance %): 480 (100), 478 (100), 462 (8), 460 (8.3), 300 (18), 298 (19), 179 (12.5); matrix-assisted laser desorption ionization ions, *m/z* 478.5 $(M)^+$, 480.5; electrospray ionization/tandem mass spectrometry, parent ion mass: 480, 478; daughter ion masses (intensity, percentage): 462 (74), 460 (52.5), 447 (21), 445 (16.6), 431 (83.3), 429 (66.6), 300 (79), 298 (74.7), 193 (11), 191 (23.5), 179 (100).

Cell Culture. HeLa cells were grown in Dulbecco's modified Eagle's medium supplemented with 10% fetal bovine serum (FBS) [the medium and serum were both purchased from Invitrogen (Carlsbad, CA), as were the following media and sera]. MCF-7, DU 145, and Caco-2 cells were grown in Eagle's minimum essential medium supplemented with 10% FBS and nonessential amino acids. Ca Ski, 1A9, 1A9/PTX10, 1A9/PTX22, 1A9/A8, and A2780/AD10 cells were grown in RPMI 1640 medium supplemented with 10% FBS. SigC and T84 cells were grown in Dulbecco's modified Eagle's medium/Ham's F-12 (1:1) medium supplemented with 10% FBS. SK-OV-3 cells were grown in McCoy's 5a medium supplemented with 10% FBS, and MDA-MB-231 cells were grown in L-15 medium supplemented with 10% FBS. All cells were grown as monolayers in tissue culture plates or on glass coverslips at 37°C in a 5% CO_2/95% air atmosphere. The 1A9 cell line is a clone of the human ovarian carcinoma cell line A2780. The two paclitaxel-resistant cell lines 1A9/PTX10 and 1A9/PTX22 and the epothilone-resistant cell line 1A9/A8 were derived from 1A9 as described previously (Giannakakou et al., 1997, 2000). The multidrug-resistant cell line A2780/AD10 was also derived from A2780 (Pryor et al., 2002).

Tubulin Binding Assay. Fluorescence titration for determining the tubulin binding parameters was performed as described previously (Peyrot et al., 1992). In brief, noscapine, 5-Br-nosc, and Rd 5-Br-nosc (0–100 μM) were incubated with 2 μM tubulin in 25 mM PIPES, pH 6.8, 3 mM $MgSO_4$, and 1 mM EGTA for 45 min at 37°C. The relative intrinsic fluorescence intensity of tubulin was then monitored in a JASCO FP-6500 spectrofluorometer (JASCO, Tokyo, Japan) using a cuvette of 0.3-cm path length, and the excitation wavelength was 295 nm. The fluorescence emission intensity of noscapine and its derivatives at this excitation wavelength was negligible. A 0.3-cm path-length cuvette was used to minimize the inner filter effects caused by the absorbance of these agents at higher concentration ranges. In addition, the inner filter effects were corrected using a formula $F_{corrected} = F_{observed}$.antilog $[(A_{ex} + A_{em})/2]$, where A_{ex} is the absorbance at the excitation wavelength and A_{em} is the absorbance at the emission wavelength. The dissociation constant (K_d) was determined by the formula: $1/B = K_d/[\text{free ligand}] + 1$, where B is the fractional occupancy and [free ligand] is the concentration of free noscapine, 5-Br-nosc, or Rd 5-Br-nosc. The fractional occupancy (B) was determined by the formula $B = \Delta F/\Delta F_{max}$, where ΔF is the change in fluorescence intensity when tubulin and its ligand are in equilibrium and ΔF_{max} is the value of maximum fluorescence change when tubulin is completely bound with its ligand. ΔF_{max} was calculated by plotting $1/\Delta F$ versus 1/liter using total ligand concentration as the first estimate of free ligand concentration.

Tubulin Polymerization Assay. Spectrophotometer cuvettes (0.4-cm path length) held a solution consisting of microtubule assembly buffer (100 mM PIPES, 2 mM EGTA, 1 mM $MgCl_2$, 1 mM GTP, pH 6.8) and 10 or 100 μM noscapine, 10 or 100 μM 5-Br-nosc, 10 or 100 μM Rd 5-Br-nosc, 10 μM paclitaxel, 10 μM nocodazole, or the solvent DMSO. Cuvettes were kept at room temperature before the addition of 10 μM purified tubulin and shifted to 37°C in a temperature controlled Ultrospec 3000 spectrophotometer (Pharmacia Biotech, Cambridge, UK). The assembly was monitored by measuring the changes in absorbance (350 nm) at 0.5-min intervals.

Measurement of Insoluble and Soluble Tubulin. Cells were washed with phosphate-buffered saline (PBS), and soluble proteins were then extracted under conditions that prevent microtubule depolymerization (0.1% Triton X-100, 0.1 M *N*-morpholinoethanesulfonic acid, pH 6.75, 1 mM $MgSO_4$, 2 mM EGTA, 4 M glycerol). The remaining cytoskeletal fraction in the culture dish was dissolved in 0.5 ml of 0.5% SDS in 25 mM Tris, pH 6.8. Total protein concentration was then determined in each fraction by BCA reagents (Pierce, Rockford, IL). Equivalent amounts for each treatment group were loaded for SDS/polyacrylamide gel electrophoresis. The proteins were then electrophoretically transferred for Western blot analysis using a mouse monoclonal anti-α-tubulin antibody (DM1A; Sigma) and a horseradish peroxidase-conjugated anti-mouse secondary antibody (Jackson ImmunoResearch, West Grove, PA). Tubulin bands were visualized using enhanced chemiluminescence following the manufacturer's instructions (Amersham Biosciences, Piscataway, NJ), and their relative levels were determined by densitometric analysis using a Lynx video densitometer (Biological Vision Inc., San Mateo, CA).

Flow Cytometric Analysis. The flow cytometric evaluation of the cell cycle status was performed as described previously (Zhou et al., 2002b). Briefly, 2×10^6 HeLa cells were centrifuged, washed twice with ice-cold PBS, and fixed in 70% ethanol. Tubes containing the cell pellets were stored at −20°C for at least 24 h. After this, the cells were centrifuged at 1000*g* for 10 min and the supernatant was discarded. The pellets were resuspended in 30 μl of phosphate/citrate buffer (0.2 M Na_2HPO_4/0.1 M citric acid, pH 7.5) at room temperature for 30 min. Cells were then washed with 5 ml of PBS and incubated with propidium iodide (PI, 20 μg/ml)/RNase A (20 μg/ml) in PBS for 30 min. Samples were analyzed on a Coulter Elite flow cytometer (Beckman Coulter, Inc., Fullerton, CA).

Immunofluorescence Microscopy. Cells were grown on poly(L-lysine)-coated glass coverslips for immunofluorescence microscopy as described previously (Zhou et al., 2002b, 2002c). To visualize microtubules, cells were fixed with methanol for 5 min at −20°C, processed with a mouse monoclonal anti-α-tubulin antibody (DM1A diluted 1000-fold, Sigma) followed by a fluorescein isothiocyanate (FITC)-conjugated anti-mouse secondary antibody (diluted 100-fold; Jackson ImmunoResearch). Cells were stained with PI (0.5 μg/ml) for 30 s at room temperature to visualize DNA. Coverslips were

mounted with AquaMount (Lerner Laboratories, Pittsburgh, CA) containing 0.01% 1,4-diazobicyclo(2,2,2)octane (Sigma) and examined with a Zeiss Axiovert 135 fluorescence microscope using 100×/1.3 numerical aperture oil lens (Plan-Neofluar; Carl Zeiss Inc., Thornwood, NY). To visualize Mad2, cells were fixed with 1% paraformaldehyde in PBS for 20 min at room temperature, permeabilized with 0.2% Triton X-100/PBS for 2 min, and then incubated with a rabbit polyclonal anti-Mad2 antibody (a kind gift from Dr. E. D. Salmon, University of North Carolina, diluted 200-fold) followed by a FITC-conjugated anti-rabbit secondary antibody (diluted 100-fold, Jackson ImmunoResearch). Cells were then counterstained with PI, mounted, and examined as described above.

Measurement of Sister Kinetochore Distance. Cells grown on poly(L-lysine)-coated glass coverslips were fixed with 2% paraformaldehyde in PBS, permeabilized with 0.2% Triton X-100/PBS, and then incubated with a mouse monoclonal anti-α-tubulin antibody (DM1A diluted 1000-fold; Sigma) and a human serum that recognizes kinetochores (diluted 1000-fold; a generous gift from Dr. K. F. Sullivan, Scripps Research Institute, La Jolla, CA). Cells were then incubated with rhodamine-conjugated anti-mouse and FITC-conjugated anti-human secondary antibodies (both diluted 100-fold; Jackson ImmunoResearch) and mounted as described above. All images were taken from the stacks of 12-bit confocal images using the LSM510 imaging software (Carl Zeiss), and the center-to-center distance between paired kinetochores was measured as described previously (Zhou et al., 2002b). When sister kinetochores were in the same focal plane, the real distance between them (d) equals the measured distance (y). When sister kinetochores were not in the same focal plane, the real distance between them (d) was corrected by triangulation of the measured distance (y) and the z-axis distance (z) between two focal planes containing the brightest staining for each of the two sister kinetochores ($d^2 = y^2 + z^2$).

In Vitro Cell Proliferation Assay. The cell proliferation assay was performed in 96-well plates as described previously (Skehan et al., 1990; Zhou et al., 2002a). In brief, 2×10^3 cells were seeded in each well and incubated with gradient concentrations of noscapine, 5-Br-nosc, or Rd 5-Br-nosc for 72 h. The cells were then fixed with 50% trichloroacetic acid and stained with 0.4% sulforhodamine B dissolved in 1% acetic acid. The cells were then washed with 1% acetic acid to remove unbound dye. The protein-bound dye was extracted with 10 mM Tris base to determine the optical density at 564-nm wavelength using a SPECTRAmax PLUS 384 microplate spectrophotometer (Molecular Devices, Sunnyvale, CA).

Results

5-Br-nosc and Rd 5-Br-nosc Have Higher Tubulin Binding Activity than Noscapine. Tubulin, like many other proteins, contains considerable aromatic amino acids, such as tryptophan, giving tubulin an intrinsic fluorescence. Tubulin-binding agents typically quench the fluorescence emission spectrum of tubulin in a concentration-dependent manner (Peyrot et al., 1992; Panda et al., 1997; Ye et al., 1998). This provides a basis for using the fluorescence titration method to determine the dissociation constant (K_d) between tubulin and its binding agents. We found that noscapine, 5-Br-nosc, and Rd 5-Br-nosc all quenched tubulin fluorescence in a concentration-dependent manner (Fig. 1, B, E, and H). The dissociation constant (K_d) was determined by the formula: $1/B = K_d/[\text{free ligand}] + 1$, where B is the fractional occupancy, and [free ligand] is the concentration of free noscapine, 5-Br-nosc, or Rd 5-Br-nosc (Fig. 1, C, F, and I). This analysis gave a dissociation constant (K_d) of 144 ± 2.8 μM for noscapine binding to tubulin, 54 ± 9.1 μM for 5-Br-nosc binding to tubulin, and 106 ± 4.2 μM for Rd 5-Br-nosc binding to tubulin. These results thus indicate that 5-Br-nosc and Rd 5-Br-nosc have higher tubulin binding activity than noscapine. We also examined the tubulin binding activity of reduced noscapine as a control for Rd 5-Br-nosc and could not obtain a dissociation constant because the effect of reduced noscapine on tubulin fluorescence was minimal (data not shown).

Effects of 5-Br-nosc and Rd 5-Br-nosc on the Assembly of Tubulin Subunits. We have previously shown that noscapine, although binding to tubulin, does not significantly promote or inhibit microtubule polymerization, even at a concentration as high as 100 μM; instead, it alters the steady-state dynamics of microtubule assembly primarily by increasing the amount of time that the microtubules spend in an attenuated (pause) state (Zhou et al., 2002b). This unique property of noscapine has led to its successful use in exploring the role of microtubule dynamics during the spindle assembly checkpoint signaling (Zhou et al., 2002b). In this study, we examined the effects of 5-Br-nosc and Rd 5-Br-nosc on the assembly of tubulin subunits into microtubules in vitro by measuring the changes in the turbidity produced upon tubulin polymerization (Fig. 2). As expected, 10 μM paclitaxel strongly promoted tubulin polymerization into microtubules, and 10 μM nocodazole strongly inhibited tubulin polymerization (Fig. 2). In addition, consistent with our previous observation (Zhou et al., 2002b), 10 or 100 μM noscapine did not have a significant effect on tubulin polymerization. 10 μM 5-Br-nosc or Rd 5-Br-nosc did not have a significant effect on tubulin polymerization, either. However, at 100 μM, both 5-Br-nosc and Rd 5-Br-nosc inhibited tubulin polymerization, although the effect of Rd 5-Br-nosc was not as obvious as that of 5-Br-nosc (Fig. 2).

Effects of 5-Br-nosc and Rd 5-Br-nosc on the Cellular Levels of Insoluble versus Soluble Tubulin. To test the effects of 5-Br-nosc and Rd 5-Br-nosc on tubulin polymerization in cells, we prepared cell extracts that contains insoluble and soluble tubulin, respectively, from HeLa cells treated with these agents (Fig. 3). An equivalent amount of the solvent DMSO was used as a control, and 10 or 100 μM noscapine, 10 μM paclitaxel, and 10 μM nocodazole were also used as comparisons. We found that the percentage of insoluble tubulin in cells treated with the solvent DMSO was 61.5% (control, Fig. 3). For cells treated with 10 μM paclitaxel, 99.2% of tubulin was in the insoluble form, and for

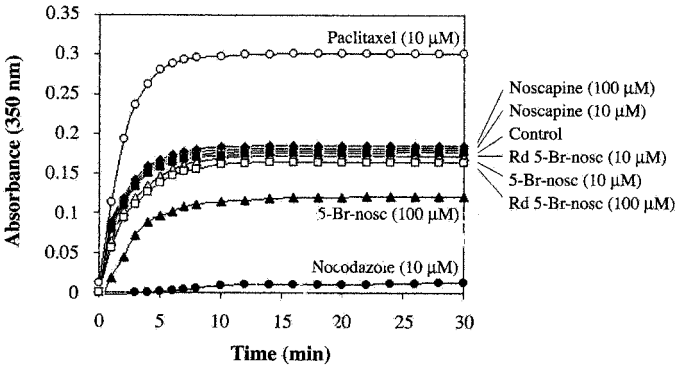

Fig. 2. Effects of noscapine, 5-Br-nosc, and Rd 5-Br-nosc on the assembly of tubulin into microtubules in vitro. The assay was based on the light scattering ability of tubulin polymer, reflected as the absorbance at 350 nm wavelength. An equivalent amount of the solvent DMSO was used as a control, and 10 μM paclitaxel and nocodazole were also used for comparisons.

those cells treated with 10 μM nocodazole, only 9.8% of the tubulin was insoluble (Fig. 3). However, the percentage of insoluble tubulin in cells treated with 10, 100 μM noscapine, 10 μM 5-Br-nosc, and 10 μM Rd 5-Br-nosc was 60.5, 59.8, 60.2, and 60.9%, respectively, which were very similar to that in the control cells (Fig. 3). Consistent with the inhibitory effect of high-dose 5-Br-nosc on tubulin polymerization (Fig. 2), the percentage of insoluble tubulin in cells treated with 100 μM 5-Br-nosc was 37.6%. In contrast, the percentage of insoluble tubulin in 100 μM Rd 5-Br-nosc treated cells was 59.7%, which was only slightly lower than that in the control cells (Fig. 3).

5-Br-nosc and Rd 5-Br-nosc Are More Active than Noscapine in Arresting Mitosis. Because all known microtubule-interfering agents, including noscapine (Ye et al., 1998, 2001; Zhou et al., 2002b, 2002a), are able to arrest mitosis in mammalian cells (Jordan and Wilson, 1999), we examined the effects of 5-Br-nosc and Rd 5-Br-nosc on cell cycle progression and compared with the effect of noscapine. We used HeLa cells because they are known to have a tight spindle assembly checkpoint (Skoufias et al., 2001; Zhou et al., 2002b). We found that the percentage of mitotic cells (the mitotic index) was increased in a concentration-dependent manner upon treatment with noscapine, 5-Br-nosc, and Rd 5-Br-nosc for 24 h (Fig. 4A). The concentration needed to arrest 50% of HeLa cells at mitosis was 18.4 μM for noscapine, as determined by the curve of mitotic index versus drug concentration. In contrast, only 7.7 and 3.6 μM were required, respectively, for 5-Br-nosc and Rd 5-Br-nosc to arrest 50% of cells at mitosis (Fig. 4A), indicating that they are more active than noscapine in arresting mitosis. The higher activity of 5-Br-nosc and Rd 5-Br-nosc in arresting mitosis was further confirmed by flow cytometric analysis of DNA content. For example, the fraction of cells in G_2/M, which have duplicated (4N) DNA content, was 15.2, 51.8, and 72.7%, respectively, upon treatment with 6.4 μM noscapine, 5-Br-nosc, and Rd 5-Br-nosc for 24 h (Fig. 4B).

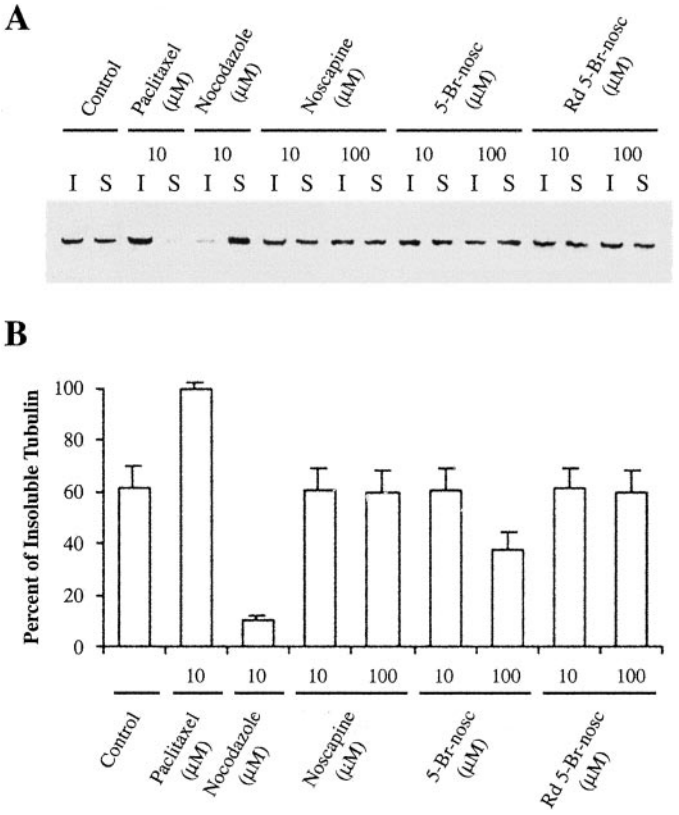

Fig. 3. Effects of noscapine, 5-Br-nosc, and Rd 5-Br-nosc on the levels of insoluble versus soluble tubulin in HeLa cells. A, Western blot analysis showing the levels of insoluble (I) and soluble (S) tubulin in cells treated for 4 h with 10 or 100 μM noscapine, 10 or 100 μM 5-Br-nosc, 10 or 100 μM Rd 5-Br-nosc, 10 μM paclitaxel, 10 μM nocodazole, or an equivalent amount of the solvent DMSO as a control. The preparation of cell extracts that contain insoluble and soluble tubulin, respectively was described under *Materials and Methods*. B, quantitation of the percentage of insoluble tubulin in cells treated as described above by densitometry. Values and error bars shown in this graph represent the averages and standard deviations, respectively, of three independent experiments.

We examined the morphology of HeLa cells arrested by 5-Br-nosc and Rd 5-Br-nosc and compared it with noscapine-arrested cells as well as normal interphase, prometaphase, and metaphase cells. Microtubules existed as a radial array in normal interphase cells and they formed a bipolar apparatus, the mitotic spindle, in mitosis (Fig. 4C). Consistent with our previous observation (Zhou et al., 2002b), noscapine-arrested HeLa cells had nearly normal bipolar spindles but did not complete chromosome alignment; some chromosomes were aligned at the equatorial plane, whereas the rest remained near the spindle poles. In contrast, cells arrested by 5-Br-nosc and Rd 5-Br-nosc had multipolar spindles (Fig. 4C). Furthermore, the multipolar spindle morphology existed even in cells arrested by high concentrations (e.g., 100 μM) of 5-Br-nosc and Rd 5-Br-nosc (data not shown).

Impairment of Chromosome Attachment to Kinetochore Microtubules by Noscapine, 5-Br-nosc, and Rd 5-Br-nosc. The abnormal spindle morphology in cells arrested by noscapine, 5-Br-nosc, and Rd 5-Br-nosc suggested that the attachment of chromosomes to kinetochore microtubules might be disrupted. To test this, we examined the localization patterns of Mad2, a spindle assembly checkpoint protein known to be essential for sensing the attachment of chromosomes to kinetochore microtubules in human cells (Li and Benezra, 1996). In prometaphase, Mad2 was localized to the kinetochore region, whereas in metaphase, it was no longer detectable at kinetochores (Fig. 5). In noscapine-arrested mitotic cells, Mad2 was present at the kinetochores on chromosomes that were near the spindle poles but was not detectable on chromosomes aligned at the equatorial plane (Fig. 5; also see Zhou et al., 2002b). In cells arrested by 5-Br-nosc and Rd 5-Br-nosc, Mad2 signal could be seen at the kinetochores on most chromosomes (Fig. 5). These results indicate that noscapine, 5-Br-nosc, and Rd 5-Br-nosc disrupt the attachment of chromosomes to kinetochore microtubules.

Comparable Impairment of Kinetochore Tension by Noscapine, 5-Br-nosc, and Rd 5-Br-nosc. When the sister chromatids become attached to kinetochore microtubules from two opposite spindle poles, tension develops across the sister kinetochores because of the mitotic force that tends to pull the chromatids toward two opposite spindle poles against the glue (cohesin) that holds the sister chromatids together (Mitchison and Salmon, 1992; Rieder and Salmon, 1994; Nicklas, 1997). The tension across sister kinetochores, apparent as a visible increase in the distance between them, is believed to be crucial for the spindle assembly checkpoint signaling in organisms from yeast to humans (Nicklas, 1997; Zhou et al., 2002d). We thus asked whether the spindle

defects caused by noscapine, 5-Br-nosc, and Rd 5-Br-nosc were associated with impaired kinetochore tension.

We examined kinetochore tension by measuring the distance between paired kinetochores. Immunofluorescent staining followed by confocal microscopy allowed us to clearly resolve the paired kinetochores on sister chromatids (Fig. 6A, insets). The distance between sister kinetochores in normal metaphase HeLa cells was measured to be 1.91 ± 0.41 μm on average (Fig. 6B), which was in agreement with those reported previously (Skoufias et al., 2001; Zhou et al., 2002b). In contrast, in cells arrested by noscapine, 5-Br-nosc, and Rd 5-Br-nosc, the average sister kinetochore distance was measured to be 1.32 ± 0.39 μm (30.9% reduction), 1.28 ± 0.36 μm (33.0% reduction), and 1.26 ± 0.41 μm (34.0% reduction), respectively (Fig. 6B). The comparable extents of reduction in the sister kinetochore distance by noscapine, 5-Br-nosc, and Rd 5-Br-nosc indicate that they impair kinetochore tension to similar degrees.

5-Br-nosc and Rd 5-Br-nosc Are More Potent than Noscapine in Inhibiting the Proliferation of Human Cancer Cells. We then performed in vitro cell proliferation assays to examine the effects of noscapine, 5-Br-nosc, and Rd 5-Br-nosc on the proliferation of a series of human cancer cell lines. They included human breast cancer cell lines MCF-7 and MDA-MB-231, cervical cancer cell lines HeLa and Ca Ski, colon cancer cell lines Caco-2 and T84, ovarian cancer cell lines SK-OV-3 and SigC, and a prostate cancer cell line, DU 145 (Fig. 7A). We found that 5-Br-nosc and Rd 5-Br-nosc inhibited the proliferation of these human cancer cell lines more efficiently than noscapine, as reflected by the much lower IC_{50} values, the drug concentrations needed to prevent cell proliferation by 50% (Fig. 7A). For example, the IC_{50} values of noscapine, 5-Br-nosc, and Rd 5-Br-nosc were 33.4 ± 3.7, 5.8 ± 1.1, and 3.8 ± 0.5 μM, respectively for MCF-7 cells, and 34.8 ± 3.1, 3.9 ± 0.8, and 2.2 ± 0.7 μM, respectively for DU 145 cells (Fig. 7A). The significantly lower IC_{50} values suggest that 5-Br-nosc and Rd 5-Br-nosc are more potent than noscapine in inhibiting the proliferation of human cancer cells.

We also examined the effects of noscapine, 5-Br-nosc, and Rd 5-Br-nosc on the proliferation of a set of human ovarian cancer cells sensitive or resistant to paclitaxel and epothilone (Fig. 7B). These included the parent cell line 1A9 (a clone of line A2780) and four drug-resistant cell lines, including two paclitaxel-resistant cell lines (1A9/PTX10 and 1A9/PTX22), an epothilone-resistant cell line (1A9/A8), and a multidrug-resistant cell line (A2780/AD10). 1A9/PTX10, 1A9/PTX22, and 1A9/A8 were derived from 1A9 and they harbor β-tubulin mutations that confer resistance to paclitaxel or epothilone (Giannakakou et al., 1997, 2000). A2780/AD10 cells were also derived from A2780 and they overexpress P-glycoprotein producing a multidrug resistance phenotype (Pryor

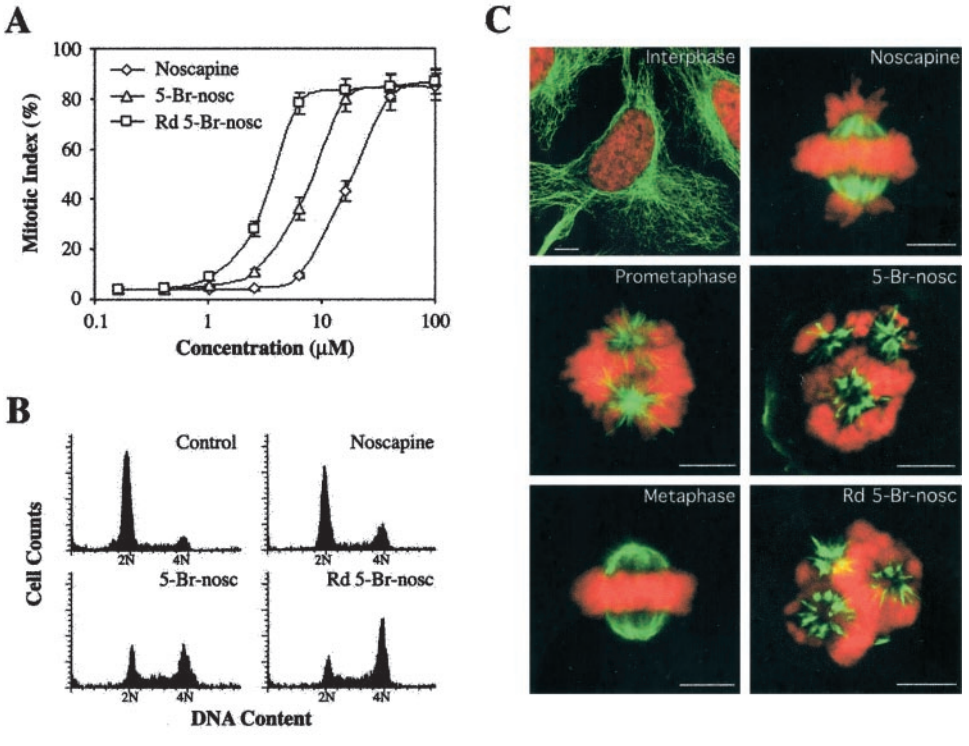

Fig. 4. 5-Br-nosc and Rd 5-Br-nosc are more active than noscapine in arresting mitosis and they cause spindle abnormalities differently from noscapine. A, mitotic indices of HeLa cells after treatment with gradient concentrations of noscapine, 5-Br-nosc, and Rd 5-Br-nosc for 24 h. B, flow cytometric analysis of DNA content in control HeLa cells and in cells treated with 6.4 μM noscapine, 5-Br-nosc, or Rd 5-Br-nosc. C, immunofluorescence micrographs of microtubule arrays (green) and DNA (red) in control interphase, prometaphase, and metaphase HeLa cells and in cells arrested by noscapine, 5-Br-nosc, and Rd 5-Br-nosc at the concentrations needed to arrest 50% of the cells at mitosis (18.4, 7.7, and 3.6 μM, respectively). Note that noscapine-arrested cells have nearly normal bipolar spindles whereas cells arrested by 5-Br-nosc or Rd 5-Br-nosc have multipolar spindles. Scale bar, 10 μm.

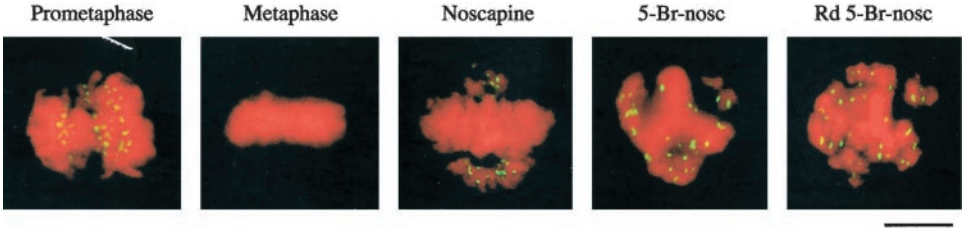

Fig. 5. Noscapine, 5-Br-nosc, and Rd 5-Br-nosc affect kinetochore-microtubule attachment as revealed by the presence of Mad2 (green) at the kinetochores on the chromosomes (red). Cells arrested by 18.4 μM noscapine, 7.7 μM 5-Br-nosc, and 3.6 μM Rd 5-Br-nosc were compared with control prometaphase and metaphase cells. Scale bar, 10 μm.

et al., 2002). We found that noscapine effectively inhibited the proliferation of 1A9, 1A9/PTX10, 1A9/PTX22, 1A9/A8, and A2780/AD10 cells (Fig. 7B). Furthermore, 5-Br-nosc and Rd 5-Br-nosc were more active than noscapine in inhibiting the proliferation of these drug-resistant cancer cell lines, as indicated by their much lower IC_{50} values (Fig. 7B).

Discussion

Microtubule-interfering agents have played an important role in early experiments studying the basic mechanisms of mitosis. This is primarily because of their ability to interfere with spindle microtubules and halt cell cycle progression at mitosis. In fact, the subunit of microtubules, tubulin, was first identified as a high-affinity colchicine receptor located on the mitotic apparatus (Weisenberg et al., 1968). In addition, the major components involved in the spindle assembly checkpoint were identified in budding yeast for mutants that fail to arrest in mitosis in the presence of microtubule-interfering agents (Li and Murray, 1991; Hoyt et al., 1991). We have recently found that noscapine is a unique antimicrotubule agent that alters microtubule dynamics without affecting the total polymer mass of tubulin and have successfully used it in probing the spindle assembly checkpoint mechanisms (Zhou et al., 2002b). In this study, we demonstrate that two brominated derivatives of noscapine, 5-Br-nosc and reduced Rd 5-Br-nosc, have higher tubulin binding activity than noscapine and affect tubulin polymerization differently from noscapine. To facilitate the use of 5-Br-nosc and Rd 5-Br-nosc in studying mitotic processes, it will be of great importance to investigate their effects on the dynamic instability parameters of microtubule assembly.

In this study, we demonstrate that 5-Br-nosc and Rd 5-Br-nosc are able to arrest cell cycle progression at mitosis at concentrations much lower than noscapine. In addition, although noscapine-arrested cells have nearly normal bipolar spindles, cells arrested by 5-Br-nosc and Rd 5-Br-nosc form multipolar spindles. The multipolar spindle morphology is intriguing, because it suggests that 5-Br-nosc and Rd 5-Br-nosc might also affect the centrosome, which tethers the minus ends of spindle microtubules and is critical for spindle morphogenesis in most cells. We show that the inhibitory effect of 5-Br-nosc on tubulin polymerization is greater than that of Rd 5-Br-nosc. However, Rd 5-Br-nosc is in turn more active than 5-Br-nosc in arresting mitosis and inhibiting cell proliferation. These results thus support the hypothesis that the mechanisms by which microtubule-interfering agents arrest cells at mitosis and inhibit cell proliferation might lie in the suppression of spindle microtubule dynamics instead of their action on microtubule polymerization or depolymerization (Wilson and Jordan, 1995).

The spindle assembly checkpoint, as a molecular safeguard, is essential for faithful transmission of chromosomes during mitosis. The spindle assembly checkpoint examines whether prerequisites for chromosome segregation have been satisfied and thereby determines whether to execute or to delay chromosome segregation (Zhou et al., 2002d). Only when all the chromosomes are attached by kinetochore microtubules from two opposite poles and proper tension is

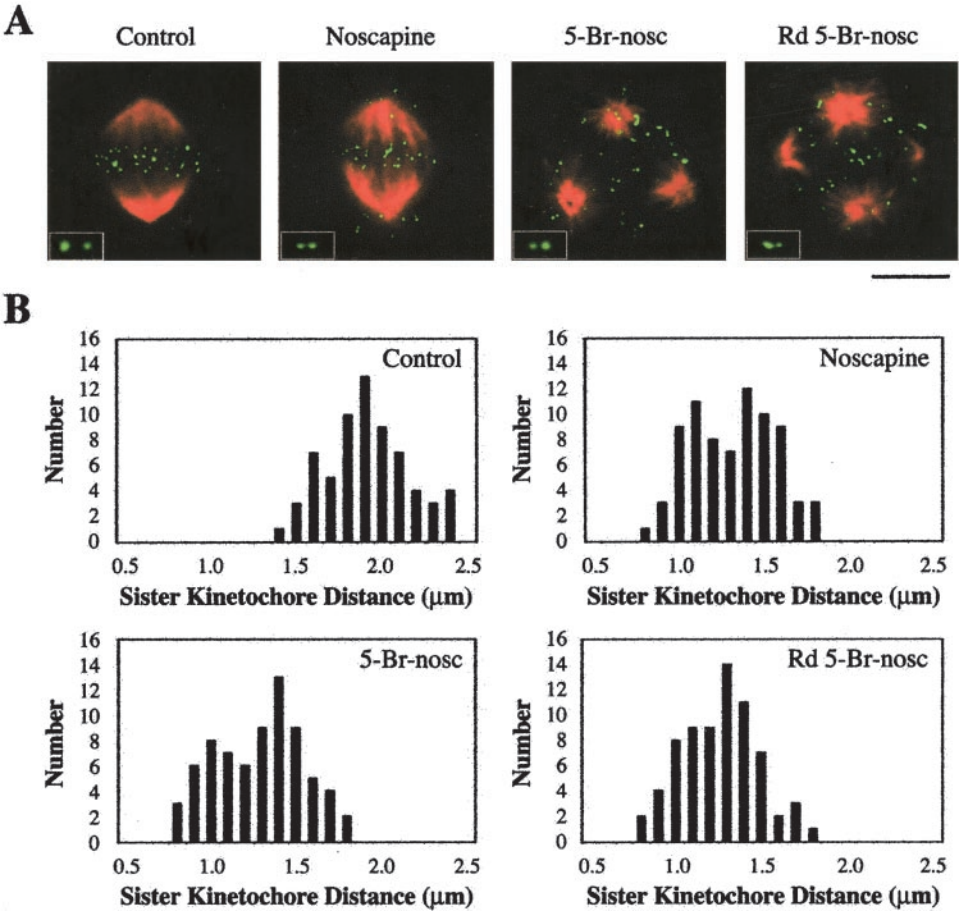

Fig. 6. Noscapine, 5-Br-nosc, and Rd 5-Br-nosc impair the tension across paired kinetochores. A, immunofluorescence micrographs showing paired kinetochores (green) and microtubules (red) in control metaphase HeLa cells and in cells arrested by 18.4 μM noscapine, 7.7 μM 5-Br-nosc, and 3.6 μM Rd 5-Br-nosc. Insets are magnified images of representative kinetochore pairs. Scale bar, 10 μm. B, noscapine and its two derivatives cause the reduction of sister kinetochore distance to similar extents, indicating that they impair kinetochore tension to similar degrees. Sister kinetochore distances were measured as described under *Materials and Methods*.

placed on the paired kinetochores does anaphase take place, allowing the physical splitting of sister chromatids. Microtubule-interfering agents, although acting on microtubules with different mechanisms, all disrupt microtubule dynamics (Jordan and Wilson, 1999), which may affect both the attachment of chromosomes to kinetochore microtubules and the tension exerted on kinetochore. It is thus not surprising that all the known microtubule-interfering agents are able to halt mitotic progression by activating the spindle assembly checkpoint (Jordan and Wilson, 1999). Consistently, noscapine, 5-Br-nosc, and Rd 5-Br-nosc act on tubulin differently and cause distinct spindle defects; however, they all affect chromosome attachment to kinetochore microtubules, as indicated by localization of Mad2 at the kinetochore region. In addition, they impair kinetochore tension to similar degrees, as indicated by similar extents of reduction in the distance between sister kinetochores. The potential of 5-Br-nosc and Rd 5-Br-nosc as biological tools for studying mitotic processes thus merits thorough evaluation.

Microtubule-interfering agents, such as paclitaxel, docetaxel, and the vinca alkaloids, have proven effective for chemotherapeutic management of human cancers (van Tellingen et al., 1992; Rowinsky, 1997; Crown and O'Leary, 2000). Unfortunately, these microtubule drugs produce a variety of side effects (Rowinsky, 1997). This is mainly because microtubules perform many other functions, such as cytoplasmic organization and axonal transport, besides their function in chromosome movement during mitosis. In addition, the clinical use of the taxoids and vinca alkaloids has been limited by the development of drug resistance contributed by P-glycoprotein overexpression (Gottesman and Pastan, 1993; Bradley and Ling, 1994), altered expression of tubulin isotypes (Burkhart et al., 2001), and other unknown mechanisms. We show that 5-Br-nosc and Rd 5-Br-nosc are more potent than noscapine in inhibiting the proliferation of a series of human breast, cervical, colon, ovarian, and prostate cancer cells. Moreover, these two brominated derivatives are also more potent than noscapine in inhibiting the proliferation of human ovarian cancer cells resistant to paclitaxel and epothilone. These findings thus indicate a great potential for the use of 5-Br-nosc and Rd 5-Br-nosc as chemotherapeutic agents for the treatment of human cancers, especially for those that are resistant to currently used microtubule drugs.

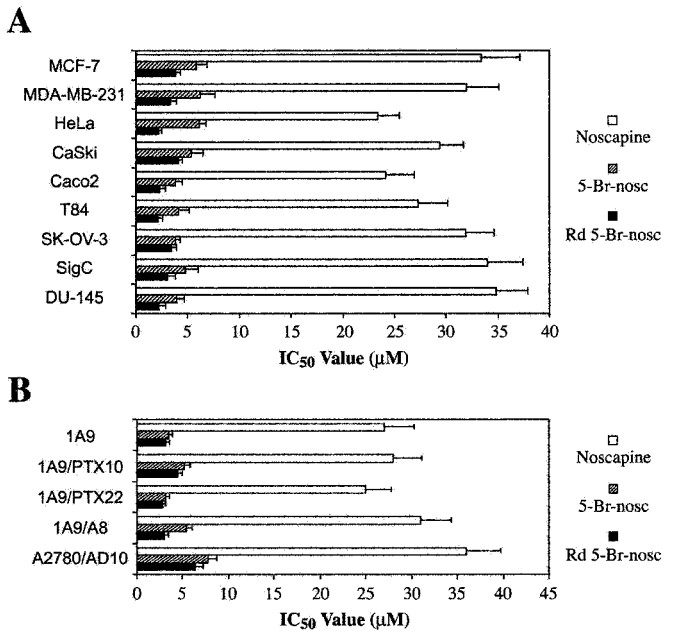

Fig. 7. 5-Br-nosc and Rd 5-Br-nosc are more active than noscapine in inhibiting the proliferation of various human cancer cells, including those that are resistant to paclitaxel and epothilone. Cells were treated with noscapine, 5-Br-nosc, and Rd 5-Br-nosc at gradient concentrations for 72 h. The IC_{50} values, which stand for the drug concentration needed to prevent cell proliferation by 50%, were then measured as described under *Materials and Methods*. Values and error bars shown in the graphs represent the averages and standard deviations, respectively, of three independent experiments. A, IC_{50} values of noscapine, 5-Br-nosc, and Rd 5-Br-nosc in human breast cancer cell lines (MCF-7 and MDA-MB-231), cervical cancer cell lines (HeLa and Ca Ski), colon cancer cell lines (Caco-2 and T84), ovarian cancer cell lines (SK-OV-3 and SigC), and a prostate cancer cell line (DU 145). B, IC_{50} values of noscapine, 5-Br-nosc, and Rd 5-Br-nosc in 1A9, a clone of human ovarian cancer cell line A2780, and four drug-resistant cell lines, including two paclitaxel-resistant cell lines (1A9/PTX10 and 1A9/PTX22), an epothilone-resistant cell line (1A9/A8), and a multidrug-resistant cell line (A2780/AD10).

Acknowledgments

We thank Drs. Edward D. Salmon and Kevin F. Sullivan for antibodies and Drs. Paraskevi Giannakakou, Rajeshwar R. Tekmal, Asma Nusrat, Robert L. Orlawski, and Ronald L. Heimark for cell lines. We also thank Drs. Ernest Hamel, Paraskevi Giannakakou, Dennis C. Liotta, James P. Snyder, and Mr. James H. Nettles for discussions. We are indebted to the anonymous reviewers of this manuscript for helpful suggestions.

References

Bradford MM (1976) A rapid and sensitive method for the quantitation of microgram quantities of protein utilizing the principle of protein-dye binding. *Anal Biochem* **72:**248–254.
Bradley G and Ling V (1994) P-glycoprotein, multidrug resistance and tumor progression. *Cancer Metastasis Rev* **13:**223–233.
Burkhart CA, Kavallaris M, and Horwitz SB (2001) The role of beta-tubulin isotypes in resistance to antimitotic drugs. *Biochim Biophys Acta* **1471:**O1–O9.
Crown J and O'Leary M (2000) The taxanes: an update. *Lancet* **355:**1176–1178.
Dahlstrom B, Mellstrand T, Lofdahl CG, and Johansson M (1982) Pharmacokinetic properties of noscapine. *Eur J Clin Pharmacol* **22:**535–539.
Desai A and Mitchison TJ (1997) Microtubule polymerization dynamics. *Annu Rev Cell Dev Biol* **13:**83–117.
Dey BB and Srinivasan TK (1935) Studies in the cotarnine series. Part IV. 5-bromonarcotine, 5-bromocotarnine, 5-bromohydrocotarnine and 5-bromonarceine and their derivatives. *J Indian Chem Soc* **12:**526–536.
Giannakakou P, Gussio R, Nogales E, Downing KH, Zaharevitz D, Bollbuck B, Poy G, Sackett D, Nicolaou KC, and Fojo T (2000) A common pharmacophore for epothilone and taxanes: molecular basis for drug resistance conferred by tubulin mutations in human cancer cells. *Proc Natl Acad Sci USA* **97:**2904–2909.
Giannakakou P, Sackett DL, Kang YK, Zhan Z, Buters JT, Fojo T, and Poruchynsky MS (1997) Paclitaxel-resistant human ovarian cancer cells have mutant β-tubulins that exhibit impaired paclitaxel-driven polymerization. *J Biol Chem* **272:**17118–17125.
Gottesman MM and Pastan I (1993) Biochemistry of multidrug resistance mediated by the multidrug transporter. *Annu Rev Biochem* **62:**385–427.
Haikala V, Sothmann A, and Marvola M (1986) Comparative bioavailability and pharmacokinetics of noscapine hydrogen embonate and noscapine hydrochloride. *Eur J Clin Pharmacol* **31:**367–369.
Hamel E and Lin CM (1981) Glutamate-induced polymerization of tubulin: characteristics of the reaction and application to the large-scale purification of tubulin. *Arch Biochem Biophys* **209:**29–40.
Hoyt MA, Totis L, and Roberts BT (1991) *S. cerevisiae* genes required for cell cycle arrest in response to loss of microtubule function. *Cell* **66:**507–517.
Jordan MA and Wilson L (1999) The use and action of drugs in analyzing mitosis. *Methods Cell Biol* **61:**267–295.
Joshi HC and Zhou J (2001) Gamma tubulin and microtubule nucleation in mammalian cells. *Methods Cell Biol* **67:**179–193.
Karlsson MO, Dahlstrom B, Eckernas SA, Johansson M, and Alm AT (1990) Pharmacokinetics of oral noscapine. *Eur J Clin Pharmacol* **39:**275–279.
Ke Y, Ye K, Grossniklaus HE, Archer DR, Joshi HC, and Kapp JA (2000) Noscapine inhibits tumor growth with little toxicity to normal tissues or inhibition of immune responses. *Cancer Immunol Immunother* **49:**217–225.
Landen JW, Lang R, McMahon SJ, Rusan NM, Yvon AM, Adams AW, Sorcinelli MD, Campbell R, Bonaccorsi P, Ansel JC, et al. (2002) Noscapine alters microtubule dynamics in living cells and inhibits the progression of melanoma. *Cancer Res* **62:**4109–4114.
Li R and Murray AW (1991) Feedback control of mitosis in budding yeast. *Cell* **66:**519–531.
Li Y and Benezra R (1996) Identification of a human mitotic checkpoint gene: hsMAD2. *Science (Wash DC)* **274:**246–248.

McIntosh JR (1994) The role of microtubules in chromosome movement, in *Microtubules* (Hyams JS and Lloyd CW eds) pp 413–434, Wiley-Liss, New York.
Mitchison TJ and Salmon ED (1992) Poleward kinetochore fiber movement occurs during both metaphase and anaphase-A in newt lung cell mitosis. *J Cell Biol* **119:**569–582.
Nicklas RB (1997) How cells get the right chromosomes. *Science (Wash DC)* **275:** 632–637.
Panda D, Chakrabarti G, Hudson J, Pigg K, Miller HP, Wilson L, and Himes RH (2000) Suppression of microtubule dynamic instability and treadmilling by deuterium oxide. *Biochemistry* **39:**5075–5081.
Panda D, Singh JP, and Wilson L (1997) Suppression of microtubule dynamics by LY290181. *J Biol Chem* **272:**7681–7687.
Peyrot V, Leynadier D, Sarrazin M, Briand C, Menendez M, Laynez J, and Andreu JM (1992) Mechanism of binding of the new antimitotic drug MDL 27048 to the colchicine site of tubulin: equilibrium studies. *Biochemistry* **31:**11125–11132.
Pryor DE, O'Brate A, Bilcer G, Diaz JF, Wang Y, Wang Y, Kabaki M, Jung MK, Andreu JM, Ghosh AK, et al. (2002) The microtubule stabilizing agent laulimalide does not bind in the taxoid site, kills cells resistant to paclitaxel and epothilones, and may not require its epoxide moiety for activity. *Biochemistry* **41:**9109–9115.
Rieder CL and Salmon ED (1994) Motile kinetochores and polar ejection forces dictate chromosome position on the vertebrate mitotic spindle. *J Cell Biol* **124:** 223–233.
Rowinsky EK (1997) The development and clinical utility of the taxane class of antimicrotubule chemotherapy agents. *Annu Rev Med* **48:**353–374.
Skehan P, Storeng R, Scudiero D, Monks A, McMahon J, Vistica D, Warren JT, Bokesch H, Kenney S, and Boyd MR (1990) New colorimetric cytotoxicity assay for anticancer-drug screening. *J Natl Cancer Inst* **82:**1107–1112.
Skoufias DA, Andreassen PR, Lacroix FB, Wilson L, and Margolis RL (2001) Mammalian mad2 and bub1/bubR1 recognize distinct spindle-attachment and kinetochore-tension checkpoints. *Proc Natl Acad Sci USA* **98:**4492–4497.
van Tellingen O, Sips JH, Beijnen JH, Bult A, and Nooijen WJ (1992) Pharmacology, bio-analysis and pharmacokinetics of the vinca alkaloids and semi-synthetic derivatives (review). *Anticancer Res* **12:**1699–1715.
Weisenberg RC, Borisy GG, and Taylor EW (1968) The colchicine-binding protein of mammalian brain and its relation to microtubules. *Biochemistry* **7:**4466–4479.
Wilson L and Jordan MA (1995) Microtubule dynamics—taking aim at a moving target. *Chem Biol* **2:**569–573.
Ye K, Ke Y, Keshava N, Shanks J, Kapp JA, Tekmal RR, Petros J, and Joshi HC (1998) Opium alkaloid noscapine is an antitumor agent that arrests metaphase and induces apoptosis in dividing cells. *Proc Natl Acad Sci USA* **95:**1601–1606.
Ye K, Zhou J, Landen JW, Bradbury EM, and Joshi HC (2001) Sustained activation of p34(cdc2) is required for noscapine-induced apoptosis. *J Biol Chem* **276:**46697–46700.
Zhou J, Gupta K, Yao J, Ye K, Panda D, Giannakakou P, and Joshi HC (2002a) Paclitaxel-resistant human ovarian cancer cells undergo c-Jun NH2-terminal kinase-mediated apoptosis in response to noscapine. *J Biol Chem* **277:**39777–39785.
Zhou J, Panda D, Landen JW, Wilson L, and Joshi HC (2002b) Minor alteration of microtubule dynamics causes loss of tension across kinetochore pairs and activates the spindle checkpoint. *J Biol Chem* **277:**17200–17208.
Zhou J, Shu HB, and Joshi HC (2002c) Regulation of tubulin synthesis and cell cycle progression in mammalian cells by gamma-tubulin-mediated microtubule nucleation. *J Cell Biochem* **84:**472–483.
Zhou J, Yao J, and Joshi HC (2002d) Attachment and tension in the spindle assembly checkpoint. *J Cell Sci* **115:**3547–3555.

Address correspondence to: Dr. Harish C. Joshi, Department of Cell Biology, Emory University School of Medicine, 615 Michael Street, Atlanta, GA 30322. E-mail: joshi@ cellbio.emory.edu